Supplementary information

Implementation of a MET in a classical wastewater treatment reactor configuration for removing nitrogen

Tejedor-Sanz, Sara[a,b], Bacchetti, Tristano[a], Salas, Juan José[c], Pastor, Laura[d] and Esteve-Núñez, Abraham[a,b]

[a] *IMDEA Water, Alcalá de Henares, Madrid, Spain*
[b] *Department of Chemical Engineering, Universidad de Alcalá de Henares, Alcalá de Henares, Madrid, Spain*
[c] *Foundation Center for New Water Technologies (CENTA), Carrión de los Césdedes, Seville, Spain*
[d] *Mediterranean Water Purification (DAM), Paterna, Valencia, Spain*

Supplementary Table 1: List of assays performed with the system and the operating conditions at each one.

Time (days)	Electrochemical condition	Operation mode	Ratio
0-7	Galvanostatic	Batch mode	-
7-17	Potentiostatic (-500 vs SHE)	Batch mode	-
18-83	Potentiostatic (-500 vs SHE)	Continuous mode	COD/N=2
84-108	Potentiostatic (-500 vs SHE)	Continuous mode	COD/N=3
109-234	Potentiostatic	Continuous mode - Study at -500 vs SHE - Study at effect of cathode polarization and different potentials - Study of factors affecting the system: role of AE, effect of O_2	COD/N=4
235-261	Potentiostatic (-500 vs SHE)	Continuous mode	COD/N=3
262-327	Potentiostatic (-500 vs SHE)	Continuous mode	COD/N=2
328-361	Potentiostatic (-500 vs SHE)	System without internal recirculation	COD/N=4

rDNA Sequencing Methodology and Analysis

A total of 3 ng of DNA were amplified with primers 515F-CS1 (ACACTGACGACATGGTTCTACA*GTGCCAGCMGCCGCGGTAA*) and 806R-CS2 (TACGGTAGCAGAGACTTGGTCT*GGACTACHVGGGTWTCTAAT*; underlined the sequencing primers, in italics the 16S rDNA-specific primers). The polymerase used was Q5 Hot Start High-Fidelity (New England Biolabs) and the PCR conditions were: initial denaturation at 98°C for 30'' followed by 30 cycles of 98°C x 10'', 60°C x 20'' and 72°C x 20'', and a final elongation step of 72°C for 2'. A 1/100 dilution of PCR products were then re-amplified (15 cycles) with Illumina´s primers AATGATACGGCGACCACCGAGATCTACACTGACGACATGGTTCTACA and CAAGCAGAAGACGGCATACGAGAT-[BC]-TACGGTAGCAGAGACTTGGTCT, where BC represent the 6 nucleotides long barcode. Positive reactions were excised out of the gel in order to get rid of any possible primer-dimers and undesired products. Finally, products were run on a Bioanalyzer (Agilent) to estimate the concentration of each simple within the region of interest and the successful generation of equimolar pools

was confirmed by qPCR. Sequencing was performed in a MiSeq equipment using the 2x250 bp format and following Illumina's protocol.

A total of around 1.000.000 sequence reads were obtained and analyzed with the QIIME 1.7 pipeline [1] with few stiches along the way. Briefly, complementary reads were merged using fastq-join [2]. Subsequently, our quality filtering strategy removed complemented sequences that had one of the following characteristics: (i) deviated more than 10 bp from the expected length (292); (ii) contained primers with more than 1 mismatch or; (iii) contained nucleotides with Phred score <20. Filtered seqs were organized in OTUs by *de novo* picking using Usearch [3] and one representative sequence per OTU was chosen. Taxonomy was assigned using the GreenGenes database[4] version 10_12 at the 97 % identity rate. Furthermore, sequences were aligned and a tree generated using FastTree 2.1.3 [5]. Finally, in order to investigate alpha diversity and the network formed by communities members with QIIME, OTUs containing less than 0.005% of the total sample reads were removed according to Bokulich [6]. The resulting network was analyzed and visualized using Cytoscape [7].

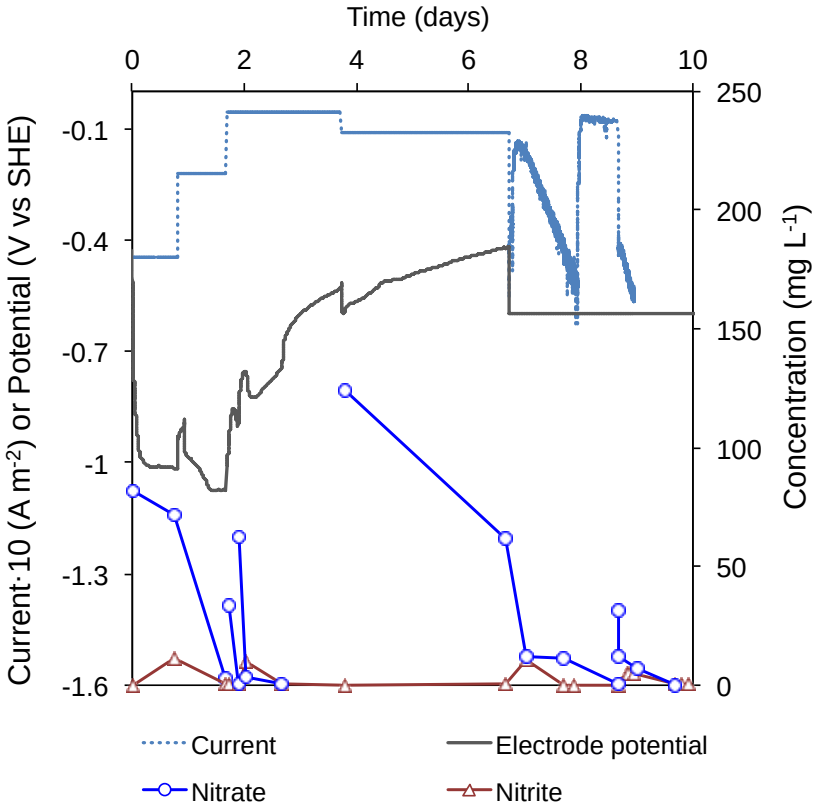

Supplementary Figure 1: Current, potential of the WE (vs SHE) and nitrogen species concentration during the start-up period at batch mode.

Supplementary Table 2: Student's t-test for each pair of variables compared. The compared variables are the ones represented in Figure 2 of the manuscript. The confidence interval was of 95 % and the significance level of 0.05.

Compared variables	Student's t	DF	Probability<t	Significant difference
% Nitrification for COD/N 2 and 3	-2.37	11	0.980	NO
% Nitrification for COD/N 3 and 4	7.854	11	1.38E-05	YES
% Nitrification for COD/N 2 and 4	4.367	11	7.03E-04	YES
% Nitrification for COD/N 4 and COD/N 4 without electrodes	6.356	8	7.12E-14	YES
% Nitrification for COD/N 4 and COD/N=4 without recirculation	12.78	8	6.62E-7	YES
% Denitrification for COD/N 2 and 3	0.744	11	0.76365	NO
% Denitrification for COD/N 3 and 4	-31.759	11	1.79E-12	YES
% Denitrification for COD/N 2 and 4	-10.533	11	2.20E-07	YES
% Denitrification for COD/N 4 and COD/N 4 without electrodes	63.106	8	9.46E-9	YES
% Denitrification for COD/N 4 and COD/N 4 without recirculation	5.20	8	4.11E-4	YES
% Total N removal for COD/N 2 and 3	-0.324	11	0.37614	NO
% Total N removal for COD/N 3 and 4	-10.935	11	1.502E-07	YES
% Total N removal for COD/N 2 and 4	-5.105	11	1.71E-04	YES
% Total N removal for COD/N 4 and COD/N 4 without electrodes	3.245	8	1.142E-2	YES
% Total N removal for COD/N 4 and COD/N 4 without recirculation	7.949	8	2.29E-5	YES

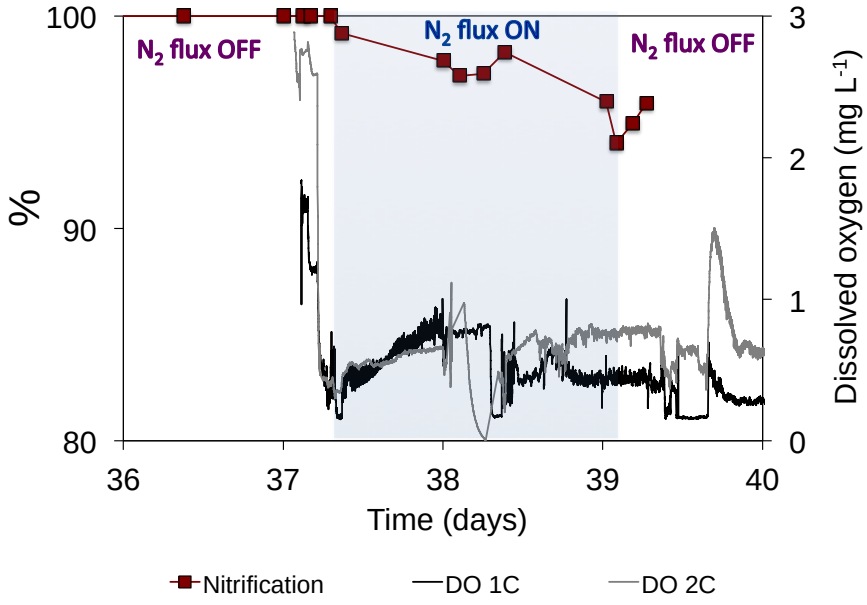

Supplementary Figure 2: Effect of removing the dissolved oxygen (DO) in the reactor over the system performance by bubbling N_2.

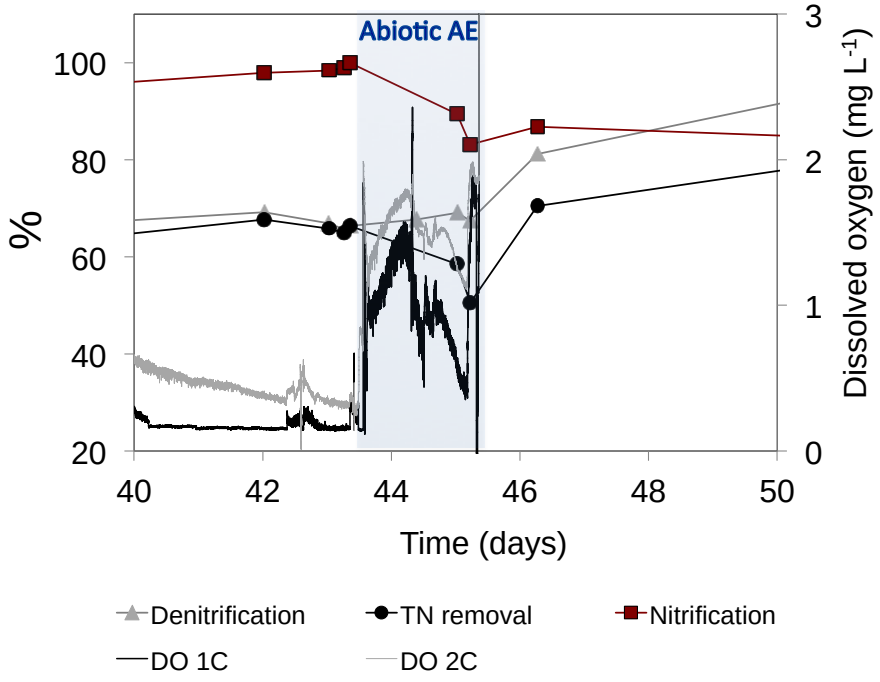

Supplementary Figure 3: Effect of the removal of the auxiliar electrode and replaced by an abiotic one of titanium.

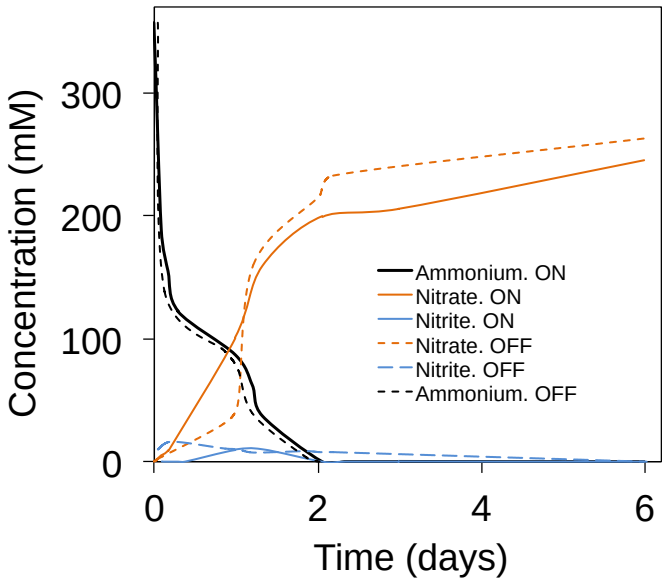

Supplementary Figure 4: Effect of the polarization of the electrodes on the nitrification process. The assay was performed at batch mode and with a medium containing ammonium and acetate at a ratio COD/N=4. ON stands for the polarization of the electrodes condition, whereas OFF stands for the open circuit potential condition.

Supplementary Figure 5: Dry sludge production during all the operation period.

Biomass density estimation on the working electrode

Biomass density estimation on the working electrode

The TG curve for the bare electrode (see Supplementary Figure 6.A) shows a single weigh loss between 25 and 1000 ^{o}C with initial temperature near 600 ^{o}C, this process shows in the STDA curve (Supplementary Figure 6.B) as a single exothermic peak. According to the literature the electrode burns in a gas-solid heterogeneous reaction mechanism, in which oxygen in the air directly oxidizes the surface of the electrode (ref?) releasing CO_2. The TG curve of the electrode with biofilm shows three weight losses. The first between 25 and 150 ºC, is associated with water loss. The second one, between 200 and 400 ºC, should be attributed to the presence of microbial matter, as it does not show in the TG curve of the bare electrode. Also, the comparative examination of the TG curves of the bare and used electrode shows that the ashes are entirely originated from the combustion of the biofilm. Thus, the percentage of dry weight of biofilm in an electrode should be the sum of the weight loss between 200 and

400 ºC and the weigh of the ashes. The mass loss attributed to the biofilm was of 1.14 mg for an electrode area of 0.075 m^2. Considering a density of 1.03 g-dry weight cm^{-3}-biofilm and a uniform thickness over the electrode area, the estimated thickness of the biofilm was of 148 μm.

The SDTA curve of the electrode with biofilm shows an exothermic peak between 200 and 400 ºC, as expected for the oxidation of the organic matter. The weight loss at 600 ºC in the TG curve appears in this curve as two small exothermic peaks in place of a single large exothermic peak shown in the STDA curve of the bare electrode. This means that the combustion of the carbon of the electrode with biofilm has a different mechanism that for the bare electrode. The profile of the SDTA curve identify the mechanism of the burning process of this electrode as a heterogeneous - homogeneous combustion[8]. The change of mechanism can probably be caused by the presence of the mineral phase coating the fibers of carbon and decreasing the oxygen diffusion from the atmosphere to the surface of the carbon preventing its direct oxidation.

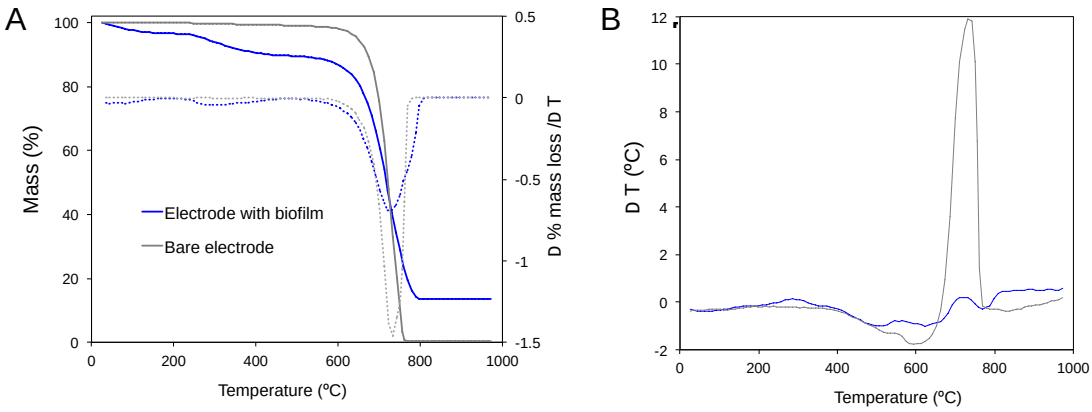

Supplementary Figure 6: A. TG profiles of both the working electrode covered with biofilm (continuous line) and a bare electrode (doted line). The black lines indicate the percentage of mass loss of the samples, and the blue lines their corresponding first derivative. B. Simulteneous Differential Thermal Analysis (SDTA) curves of the two samples

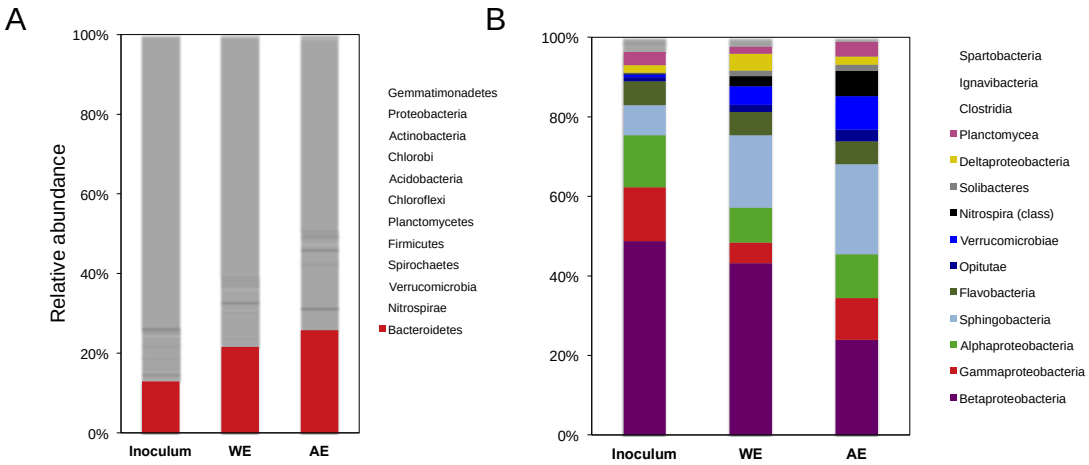

Supplementary Figure 7: Relative abundance of the different microbial communities sorted by phylum (A) and class (B) of the three samples analyzed. WE stands for the working electrode attached biomass and AE stands for the one attached to the counter electrode.

Energy demand calculations

The energy demand was calculated for the lowest system performance in terms of nitrogen removal (less current consumption due to a lower bioelectrochemical nitrate reduction), and for the highest nitrogen removal condition.

Area electrode = 0.09 m^2
Flow = 4.6 L/day
Power consumption = $\Delta E(E_{node}-E_{cathode})\cdot I_{consumed}$

- Energy consumption for COD/N=2 (lowest N removal):

Current consumption was of 0.10 A/m^2 and the nitrogen removal was of 62 % of an influent with 37 mg-N L^{-1}. The potential of the cell ($E_{anode}-E_{cathode}$) for this condition was of ca. 2.5 V.

The energy demand for this ratio was of 0.12 kWh $m^{-3}_{wastewater}$ or 0.005 kWh $g\text{-}N^{-1}$.

- Energy consumption for COD/N=4 (highest N removal):

Current consumption was of 0.39 A/m^2 and the nitrogen removal was of 81 % of an influent with 37 mg-N L^{-1}. The potential of the cell ($E_{anode}-E_{cathode}$) for this condition was of ca. 4 V.

Therefore, the estimated energy demand for this condition was of 0.7 kWh $m^{-3}_{wastewater}$ or 0.024 kWh $g\text{-}N^{-1}$.

References

1 J. G. Caporaso, J. Kuczynski, J. Stombaugh, K. Bittinger, F. D. Bushman, E. K. Costello, N. Fierer, A. G. Peña, J. K. Goodrich, J. I. Gordon, G. A. Huttley, S. T. Kelley, D. Knights, J. E. Koenig, R. E. Ley, C. A. Lozupone, D. McDonald, B. D. Muegge, M. Pirrung, J. Reeder, J. R. Sevinsky, P. J. Turnbaugh, W. A. Walters, J. Widmann, T. Yatsunenko, J. Zaneveld and R. Knight, *Nat. Methods*, 2010, 7, 335–336.

2 E. Aronesty, 2011.

3 R. C. Edgar, *Bioinformatics*, 2010, 26, 2460–2461.

4 T. Z. DeSantis, P. Hugenholtz, N. Larsen, M. Rojas, E. L. Brodie, K. Keller, T. Huber, D. Dalevi, P. Hu and G. L. Andersen, *Appl. Environ. Microbiol.*, 2006, 72, 5069–5072.

5 M. N. Price, P. S. Dehal and A. P. Arkin, *PLoS ONE*, 2010, 5, e9490.

6 N. A. Bokulich, S. Subramanian, J. J. Faith, D. Gevers, J. I. Gordon, R. Knight, D. A. Mills and J. G. Caporaso, *Nat. Methods*, 2013, 10, 57–59.

7 P. Shannon, *Genome Res.*, 2003, 13, 2498–2504.

8 Q. Li, C. Zhao, X. Chen, W. Wu and Y. Li, *J. Anal. Appl. Pyrolysis*, 2009, 85, 521–528.